Structural and Collisional Relaxations in Liquids and Supercritical Fluids

F. Bencivenga,[1] A. Cunsolo,[2] M. Krisch,[1] G. Monaco,[1] L. Orsingher,[3] G. Ruocco,[4] F. Sette,[1] and A. Vispa[5]

[1]*European Synchrotron Radiation Facility, BP 220, F-38043 Grenoble, Cedex, France*
[2]*Operative Group in Grenoble c/o ILL, CRS SOFT-INFM-CNR, BP 220, F-38043 Grenoble, Cedex, France*
[3]*Dipartimento di Fisica, Universitá di Trento, 38050 Povo, Trento, Italy*
[4]*Dipartimento di Fisica, CRS SOFT-INFM-CNR, Universitá di Roma "La Sapienza," Roma, Italy*
[5]*Dipartimento di Fisica, Universitá di Perugia, 06123 Perugia, Italy*

(Received 11 September 2006; published 20 February 2007)

The dynamic structure factor $S(Q, \omega)$ of both associated (water and ammonia) and simple fluids (nitrogen and neon) has been determined by high-resolution inelastic x-ray scattering in the 2–14 nm^{-1} momentum transfer range. A line-shape analysis with a generalized hydrodynamic model was used to study the involved relaxation process and to characterize its strength and time scale. We observe that in the liquid phase such a process is governed by rearrangements of intermolecular bonds, whereas in the supercritical region it assumes a collisional nature.

DOI: 10.1103/PhysRevLett.98.085501 PACS numbers: 63.50.+x, 61.10.Eq, 61.20.−p

High-frequency relaxation processes in liquid systems are intimately related to the details of intermolecular interactions and can give precious insights into the nature of these interactions on a microscopic level. Despite intense efforts on both the experimental and computational sides, the physical origin of these processes still eludes a comprehensive understanding concerning the microscopic driving mechanisms.

Among the various relaxations active in fluids, the so-called structural relaxation is the one related to cooperative rearrangements of the local structure consequent to external perturbations or spontaneous fluctuations [1,2]. It is characterized by a relaxation time τ_α with a strong (Arrhenius or Vogel-Fulcher) temperature dependence, which resembles the one of viscosity. It is often considered to be a sort of fingerprint of the liquid phase. In recent years, several inelastic x-ray scattering (IXS) investigations focused on hydrogen bonded (HB) liquids [3–9], revealing that the microscopic mechanism responsible for the structural relaxation process can be ascribed to the breaking and forming of the HB network.

In the supercritical phase the mechanism of making or breaking intermolecular bonds is expected to have a weaker influence on the dynamics since the thermal energy of the molecules is high as compared to the attractive interactions among them. However, no systematic investigation of the evolution of this phenomenology when the system passes from the liquid to the supercritical phase has been undertaken yet.

This motivated us to perform high statistics, high-resolution IXS measurements on various systems in the liquid and the supercritical phase. To make such a study as general as possible we compared the results achieved on both HB (water and ammonia) and non-HB (nitrogen and neon) systems in an extended portion of the thermodynamic plane [10]. The chosen samples are characterized by similar molecular masses and dimensions, while their interaction potential and molecular structure are very different.

IXS spectra have been analyzed in the framework of the generalized hydrodynamics theory, using the memory function approach [11]. This kind of analysis enables us to derive the characteristic relaxation time (τ) and strength (Δ) of the active relaxation process. We observe that τ loses its characteristic Arrhenius temperature dependence on going from liquid to supercritical conditions, and gradually becomes proportional to the value of the intercollisional time. We discuss in detail this effect and relate it to the increased relevance of harsh intermolecular repulsions (collisions) in the supercritical phase, as compared to long range interactions typical of the liquid state.

The experiment was carried out at the ID28 beam line at the ESRF in Grenoble (France). The instrument working principle is based on an extreme backscattering high-order Bragg reflection from a silicon perfect single crystal. Five independent analyzer systems, mounted at the end of a 7-m-long arm, allow the simultaneous measurement of five IXS spectra, corresponding to different momentum transfer (Q) separated by a fixed Q offset of ~ 3 nm^{-1}. The chosen experimental configuration provides an energy (momentum) transfer resolution of 1.5 meV (0.4 nm^{-1}). Ultra pure samples were loaded in specially designed high-pressure, large volume cells made of Inconel 625 with 1 mm thick diamonds as optical windows. The samples were pressurized by a manual piston and heated (cooled) by a resistor (cryostat) with a P (T) stability better than 5 bar (0.2 K). The whole setup was kept under vacuum to avoid temperature gradients as well as scattering from the air surrounding the cell. Empty cell and background measurements have been found to yield a negligible contribution to the total scattering intensity. For each thermodynamic state at least 10 IXS spectra (in the 2–14 nm^{-1} Q range) and one $S(Q)$ (in the 1–24 nm^{-1} Q range) were collected.

The line shape of the IXS spectra was described using a generalized hydrodynamic model derived within the memory function formalism. This framework has been already successfully tested in several IXS experiments on HB liquids [4–8], noble gases [12], liquid metals [13], diatomic liquids [14], supercooled molecular systems [15], and glasses [16]. Within such a framework the normalized classical dynamical structure factor $S(Q, \omega)/S(Q)$ can be written as [11]

$$\frac{S(Q,\omega)}{S(Q)} = \frac{1}{\pi} \frac{\Omega_T^2(Q) m'(Q,\omega)}{[\omega^2 - \Omega_T^2(Q) - \omega m''(Q,\omega)]^2 + \omega^2 [m'(Q,\omega)]^2}, \quad (1)$$

where $m'(Q, \omega)$ and $m''(Q, \omega)$ are the real and imaginary parts of the time Fourier transform of the memory function $m(Q, t)$, respectively. The latter was assumed to be of the following form:

$$m(Q,t) = [\gamma(Q) - 1]\Omega_T^2(Q) e^{-D_T(Q)Q^2 t} + 2\Gamma_\mu(Q) Q^2 \delta(t) + [\Omega_\infty^2(Q) - \Omega_s^2(Q)] e^{-[t\Omega_\infty^2(Q)]/[\tau_C(Q)\Omega_s^2(Q)]}, \quad (2)$$

where $D_T(Q)$, $\gamma(Q)$, $\Omega_T(Q)$, and $\Omega_s(Q) = \sqrt{\gamma(Q)}\Omega_T(Q)$ are the finite-Q generalizations of the thermal diffusivity, the specific heat ratio, and the isothermal and adiabatic sound frequency, respectively. The parameter $\Omega_T(Q)$ can also be independently calculated from the measured values of $S(Q)$, through the finite-Q generalization of the compressibility theorem [11]. The values of $\Omega_T(Q)$ obtained from these two independent procedures are in good agreement, thus providing a positive consistency check of the performed data analysis. The first term on the right-hand side of Eq. (2) accounts for the time decay of the memory function induced by the thermal diffusion process. The second one (instantaneous relaxation) accounts for the time decay of the memory function on time scales much faster than the experimentally accessed frequency window. Finally, the last term (structural relaxation) describes the time decay of the memory function induced by viscous dissipations taking place over a finite time scale: $\tau(Q) = \tau_C(Q)\Omega_s^2(Q)/\Omega_\infty^2(Q)$, where $\Omega_\infty^2(Q)$ is the high-frequency limit of the dispersion relation and τ_C is the relaxation time of the longitudinal compliance, M_L^{-1} [17]. The $t = 0$ value of this term (i.e., $\Delta(Q) = [\Omega_\infty^2(Q) - \Omega_s^2(Q)]$) is also referred to as structural relaxation strength. Such an exponential time decay of the memory function fully describes the salient features of the viscoelastic phenomenology [4–9,12–15].

The raw data have been analyzed using a standard fitting procedure based on a χ^2 minimization with the following model function: $I(Q, \omega) = Ax\{[n(x) + 1]S(Q, \omega) \otimes R(\omega)\} + B$, where $S(Q, \omega)$ is given by Eqs. (1) and (2), $R(\omega)$ is the measured instrumental resolution function, the symbol $\otimes$ stands for numerical convolution, A is an overall intensity factor, and B is an experimentally determined flat background. Finally, $n(x)$ (where $x = \hbar\omega/k_B T$) is the Bose population factor which makes the model compatible with the detailed balance principle. In the fitting routine, five parameters were free to vary, namely, A, $\Omega_T(Q)$, $\Omega_\infty(Q)$, $\tau_C(Q)$, and $\Gamma_\mu(Q)$, the amplitude of the instantaneous relaxation. The behavior of the latter parameter is not relevant for the present work, and therefore it will not be discussed. The parameters $\gamma(Q)$ and $D_T(Q)$ have been instead fixed to the corresponding thermodynamic ($Q = 0$) value, as extracted from the respective equation of state (EOS) [18], regardless of the probed Q. This choice was motivated by the lack of computational or experimental results for both variables over the rather large thermodynamic range explored by the experiment.

The good agreement between fits and experimental data can be appreciated from an inspection of Fig. 1, where selected IXS spectra of the four samples are shown and compared with the corresponding best fit line shapes (light gray lines). The logarithmic representation emphasizes the overall consistency between the model and the experimental spectra, even in the high-frequency tails. The red (dark gray) lines in the figure represent the results of an alternative fitting procedure, for which the third term in Eq. (2) has been discarded. In this case the spectrum is poorly approximated by the model, as also witnessed by the larger χ^2 values (reported in brackets). Indeed, the mismatch becomes rather evident at the low temperatures, in both the quasielastic and the inelastic shoulder regions. These observations infer the remarkable weight of the relaxation contribution to the spectrum.

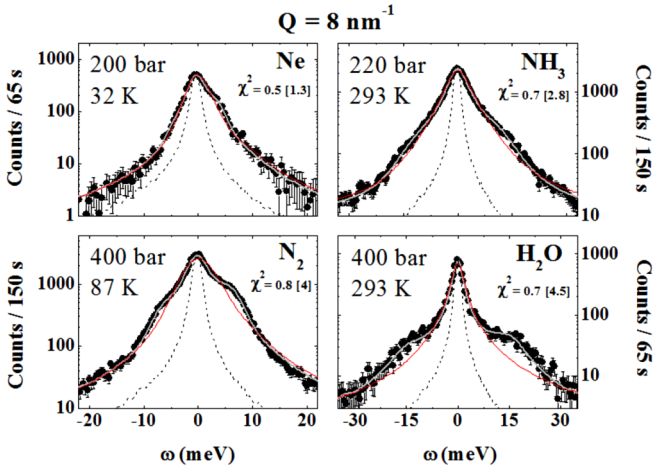

FIG. 1 (color online). Selected IXS spectra of the four samples collected at the indicated (Q, P, T) values. The thick light gray lines through the data are the best fit line shapes, while the dashed lines are the instrumental resolution functions. The corresponding χ^2 values are reported as well. The red (dark gray) lines are the results of another fitting strategy (see text); the corresponding χ^2 values are reported in brackets.

As the resulting best fit parameters are Q-dependent entities, their $Q \to 0$ limiting value has been determined by fitting their Q dependencies with an appropriate function, in order to provide a comparison between macroscopic quantities. The values obtained for the four systems are reported in Fig. 2 in an Arrhenius plot. Data belonging to the liquid phase can be described by an activation law (dashed lines in Fig. 2). This allows us to extract the activation energy (E_a) of the involved relaxation process: 11.5 ± 0.6 KJ/mole (water), 6.7 ± 0.6 KJ/mole (ammonia), and 0.3 ± 0.1 KJ/mole (nitrogen). In the case of neon, the data in the liquid phase are too few and sparse to draw any conclusion. The above values for E_a result to be similar to the energy of the respective intramolecular bonds.

Furthermore, in order to quantitatively compare data sets of different systems, a scaling parameter able to account for the different thermodynamic conditions and the different molecules under consideration is needed. A suitable choice is represented by the mean free time between intermolecular collisions, $\langle\tau\rangle$. It can be estimated by considering a hard sphere Boltzmann gas [19]:

$$\langle\tau\rangle = \frac{1}{\rho}\sqrt{\frac{1}{16\pi d^4 k_B T M}}, \tag{3}$$

where d, M, ρ, and k_B are the molecular diameter and mass, the mass density, and the Boltzmann constant, respectively. In Fig. 3 the dimensionless quantity $\tau_C/\langle\tau\rangle$ is reported as a function of T_c/T. One can readily observe that around and above T_c, the absolute value of $\tau_C/\langle\tau\rangle$ is similar in all four systems and it can be sufficiently well described by a constant function (horizontal line in Fig. 3).

The evidence that τ_C becomes proportional to $\langle\tau\rangle$ above T_c suggests that the microscopic dynamics of the system is dominated by intermolecular collisions at high temperature. On the other hand, the thermal energy of the molecules is progressively reduced while lowering the temperature, and a larger number of intermolecular bonds with a longer lifetime can be established. Below T_c the data sets of HB and non-HB systems split into two different curves, as expected owing to the different nature of the interaction potentials. In fact, a stronger attractive potential (as the one of ammonia and water) increases the lifetime of intermolecular bonds and therefore the time scale of the structural relaxation. This explains why HB systems, in contrast to nitrogen and neon, follow a pronounced exponential growth of $\tau_C/\langle\tau\rangle$. This difference disappears above T_c, where the role of attractive interactions is strongly reduced. Here the temperature dependence of the relaxation time scale becomes increasingly similar to the one of $\langle\tau\rangle$.

Finally, from the analysis of IXS spectra we can also derive the values of the relaxation strength $\Delta(Q)$. In fact, further insights into the relation between the active relaxation process and the intermolecular interactions comes from the analysis of the low-Q limit of $K(Q) = \Delta(Q)\rho/(\rho_M^2 Q^2)$, where ρ_M is the molar density. Here, the $Q \to 0$ extrapolations have been performed using a constant function. Apart from the HB systems above T_c, all the curves are more or less flat. This can be understood since $K(0)$ can be regarded as the difference between two squared sound velocities (c_∞ and c_s) that, in a first approximation, are expected to be proportional to the density in the liquid phase. The results are displayed in Fig. 4 as a function of T/T_c. It can be also noticed that the values of $K(0)$ are rather close for water and ammonia and are much higher than for nitrogen and neon. In order to have a matter of comparison among the values of $K(0)$ for different samples, one can compare them to the van der Waals pa-

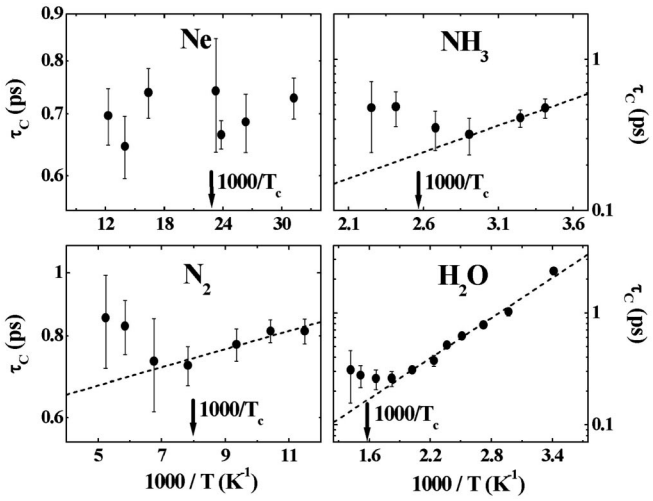

FIG. 2. $Q = 0$ extrapolated values of $\tau_C(Q)$. The lines indicate the activation behavior observed in the liquid phase.

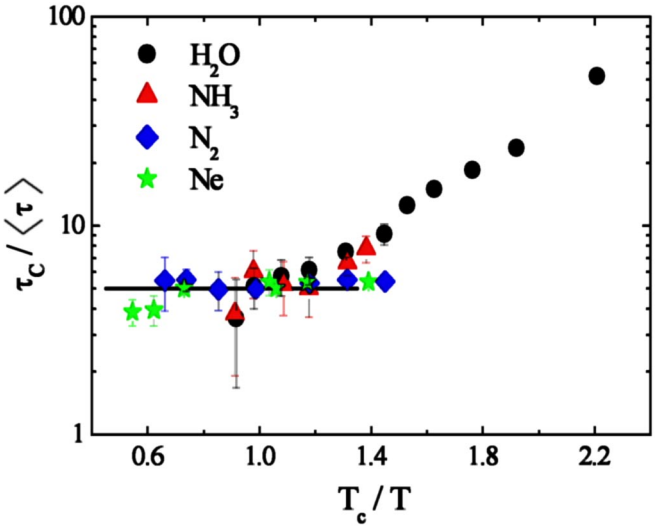

FIG. 3 (color online). Values of $\tau_C/\langle\tau\rangle$ vs T_c/T for the investigated samples. The horizontal line describes the temperature dependence of $\tau_C/\langle\tau\rangle$ above T_c.

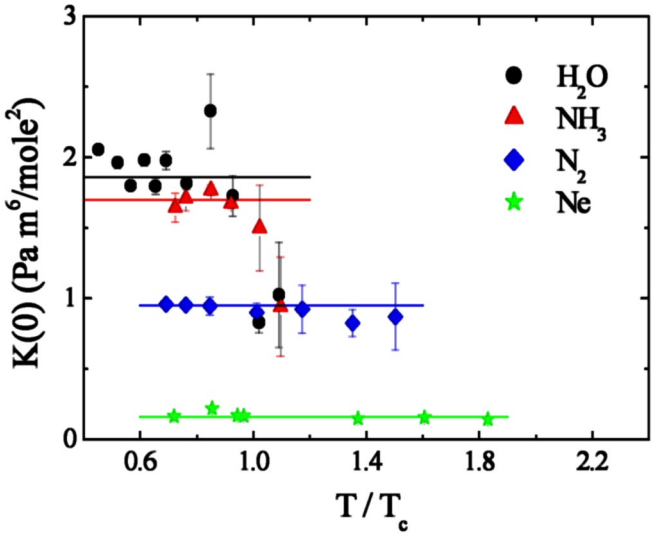

FIG. 4 (color online). Values of $K(0)$ vs T/T_c for the investigated samples. The horizontal lines are guides to the eye.

rameter a [20]. This comparison is proposed in Table I, where $\langle K(0)\rangle$ indicates the weighted average of $K(0)$.

A qualitative correlation between the two parameters can be readily noticed: the higher the $\langle K(0)\rangle$, the higher the a. As the parameter a phenomenologically quantifies the attractive intermolecular interactions in the fluid phase of a given system, it seems intuitive to infer a relationship between $K(0)$ and the degree of connectivity of the sample. This observation is consistent with the considerations made above on the T dependence of τ_C.

In conclusion, we have presented a comparative study of the evolution of the relaxation dynamics of different systems at the liquid-to-supercritical transition. From the temperature dependence of the relaxation time we observe a major change in the mechanism responsible for the active relaxation. More specifically, in the liquid phase such a mechanism can be associated with the making and breaking of intermolecular bonds, as witnessed by the (system-dependent) Arrhenius T dependence of τ_α. As soon as supercritical conditions are reached, the main interaction mechanism among molecules is represented by binary intermolecular collisions, as witnessed by the scaling of the data according to the parameter $\langle\tau\rangle$. This mechanism is the one ruling the microscopic dynamics of a fluid at moderate pressure for $T > T_c$.

TABLE I. Comparison between the van der Waals parameter a and $\langle K(0)\rangle$, the average value of $K(0)$.

	$\langle K(0)\rangle$ (Pa m^6/mole^2)	a (Pa m^6/mole^2)
Ne	0.158 ± 0.011	0.021
N_2	0.95 ± 0.12	0.136
NH_3	1.7 ± 0.2	0.423
H_2O	1.86 ± 0.13	0.551

These results provide an intuitive representation of the liquid-to-supercritical transition from a microscopic point of view since we found that, with increasing the temperature, the lifetime of intermolecular bonds decreases up to become, close to T_c, shorter than the average time between two molecular collisions. As a consequence, the time needed for a molecule to get close to another one and eventually form a new intermolecular bond becomes shorter than the average lifetime of the bond itself, thus preventing the fluid system from developing an extended bond network, typical of the liquid phase.

[1] C. A. Angell *et al.*, J. Appl. Phys. **88**, 3113 (2000).
[2] K. L. Ngai, J. Non-Cryst. Solids **275**, 7 (2000).
[3] G. Ruocco and F. Sette, J. Phys. Condens. Matter **11**, R259 (1999).
[4] G. Monaco *et al.*, Phys. Rev. E **60**, 5505 (1999).
[5] R. Angelini *et al.*, Phys. Rev. B **70**, 224302 (2004).
[6] A. Cunsolo *et al.*, Phys. Rev. Lett. **82**, 775 (1999).
[7] E. Pontecorvo *et al.*, Phys. Rev. E **71**, 011501 (2005).
[8] G. Monaco *et al.*, Phys. Rev. Lett. **82**, 1776 (1999).
[9] A. Giugni and A. Cunsolo, J. Phys. Condens. Matter **18**, 889 (2006).
[10] The explored thermodynamic states are the following. (i) Water: 11 points belonging to the isobaric line corresponding to a pressure $P = 400$ bar ($P/P_c = 1.8$), in the temperature range 293 K $\leq T \leq$ 706 K ($0.45 \leq T/T_c \leq 1.1$), corresponding to a density range of $1.1 \leq \rho/\rho_c \leq 3.2$; with the suffix "$c$" we indicate the value of the variable at the critical point. (ii) Ammonia: 6 points at $P = 220$ bar ($P/P_c = 1.9$) with 293 K $\leq T \leq$ 444 K ($0.7 \leq T/T_c \leq 1.1$) and $1.1 \leq \rho/\rho_c \leq 2.8$. (iii) Nitrogen: 7 points at $P = 400$ bar ($P/P_c = 11.8$) with 90 K $\leq T \leq$ 190 K ($0.7 \leq T/T_c \leq 1.5$ K) and $1.8 \leq \rho/\rho_c \leq 2.7$. (iv) Neon: 5 points at $P = 200$ bar ($P/P_c = 7.5$) with 32 K $\leq T \leq$ 81 K ($0.7 \leq T/T_c \leq 1.8$ K) and $1.2 \leq \rho/\rho_c \leq 2.6$; 1 point at $P = 280$ bar ($P/P_c = 10.4$) with $T = 38$ K ($T/T_c = 0.85$) and $\rho/\rho_c = 2.5$; 1 point at $P = 150$ bar ($P/P_c = 5.6$) with $T = 43$ K ($T/T_c = 0.97$) and $\rho/\rho_c = 2.2$.
[11] J. P. Boon and S. Yip, *Molecular Hydrodynamics* (McGraw-Hill International, New York, 1980).
[12] A. Cunsolo *et al.*, J. Chem. Phys. **114**, 2259 (2001).
[13] T. Scopigno *et al.*, Rev. Mod. Phys. **77**, 881 (2005).
[14] F. Bencivenga *et al.*, Europhys. Lett. **75**, 70 (2006).
[15] D. Fioretto *et al.*, Phys. Rev. E **59**, 1899 (1999).
[16] G. Ruocco *et al.*, Phys. Rev. Lett. **84**, 5788 (2000).
[17] G. Harrison, *The Dynamic Properties of Supercooled Liquids* (Academic Press, New York, 1976).
[18] Nist Database, http://webbook.nist.gov/chemistry/form-ser.html.
[19] J. O. Hirscfelder, C. F. Curtiss, and R. B. Bird, *Molecular Theory of Gases and Liquids* (John Wiley & Sons, New York, 1954).
[20] R. C. Weast, M. J. Astle, and W. H. Beyer, *CRC Handbook of Chemistry and Physics* (CRC Press, Boca Raton, 1988), 69th ed.